

Synthesis, crystal structures, and thermodynamic properties of two new lanthanide complexes

Jun-Chen Wu^{1,2} · Quan Shi³ · Li-Na Geng² · Ning Ren⁴ · Jian-Jun Zhang^{1,2}

Received: 25 May 2017 / Accepted: 28 August 2017 / Published online: 8 September 2017
© Akadémiai Kiadó, Budapest, Hungary 2017

Abstract Two new complexes [Tb(2,3-DCIBA)₃(5,5'-dmebipy)(H₂O)]₂ and [Er(2,3-DCIBA)₃(5,5'-dmebipy)(H₂O)]₂ (2,3-DCIBA = 2,3-dichlorobenzoate; 5,5'-dmebipy = 5,5'-dimethylbipyridine) were prepared and characterized by single crystal X-ray diffraction, elemental analysis, IR spectra, and TG/DSC technology. Single crystal X-ray diffraction data show that the two complexes are isomorphous. The complex is a binuclear molecular. Each Ln³⁺ center is coordinated by six oxygen atoms and two nitrogen atoms to form a distorted square antiprism geometry. The supramolecular architecture of the complex is constructed by H bond and halogen–halogen interactions. The thermal decomposition mechanism of the two complexes has been studied by TG/DSC technology. The low-temperature heat capacities of the complexes have been measured using a physical property measurement system in the temperature range from 10 to 302 K. The heat capacities were fitted to the polynomial equations by a least square method, and the

thermodynamic functions were calculated based on the curve fitting.

Keywords Lanthanide complexes · Crystal structure · Halogen–halogen interactions · Thermodynamics · Heat capacity · TG/DSC technology

Introduction

The design and synthesis of lanthanide carboxylic acids complexes have been one of the active fields for its various structures and attractive properties [1–5] and their potential applications in optical [6–11], thermodynamics [12] and magnetic fields [13–16], et al.

Lanthanide ions have high affinities for hard donor atoms such as the oxygen atom of aromatic carboxylic acid (hard acid hard base interactions) [17]. Aromatic carboxylic acid ligands (oxygen donor) have diverse coordination modes, so many supermolecules can be constructed [3, 18]. The investigation of the luminescent properties of lanthanide aromatic carboxylic acids complexes has been widely studied [19]. However, low-temperature heat capacities for these complexes have been rarely explored. Further research of heat capacities is helpful to better understand the synthesis, physical properties, and crystal structures of these lanthanide complexes.

In this paper, the synthesis and characterization of the two novel complexes [Tb(2,3-DCIBA)₃(5,5'-dmebipy)(H₂O)]₂ and [Er(2,3-DCIBA)₃(5,5'-dmebipy)(H₂O)]₂ (2,3-DCIBA = 2,3-dichlorobenzoate; 5,5'-dmebipy = 5,5'-dimethylbipyridine) are reported. The thermal decomposition mechanism of the complexes has been investigated by TG/DSC technology. The low-temperature heat capacities have been measured in the range of 10–302 K using a

✉ Ning Ren
ningren9@163.com

✉ Jian-Jun Zhang
jjzhang6@126.com

¹ Testing and Analysis Center, Hebei Normal University, Shijiazhuang 050024, Hebei, People's Republic of China

² College of Chemistry and Material Science, Hebei Normal University, Shijiazhuang 050024, Hebei, People's Republic of China

³ Thermochemistry Laboratory, Liaoning Province Key Laboratory of Thermochemistry for Energy and Materials, Dalian National Laboratory for Clean Energy, Dalian Institute of Chemical Physics, Chinese Academy of Sciences, Dalian 116023, Liaoning, People's Republic of China

⁴ College of Chemical Engineering and Material, Handan College, Handan 056005, Hebei, People's Republic of China

physical property measurement system (PPMS). The heat capacities were fitted to the polynomial equations by a least square method, and the thermodynamic functions were calculated based on the curve fitting.

Experimental

Chemicals

$\text{LnCl}_3 \cdot 6\text{H}_2\text{O}$ were obtained by the reaction of Ln_2O_3 (Beijing Lanthanide Innovation Technology Co., Ltd, 99.9%) and hydrochloric acid in aqueous solution, then evaporating liquid by water bath heating. Other reagents and solvents employed were commercially available and used without further purification.

Equipment and analytical methods

The percentage of C, H, and N in the corresponding complexes were analyzed via Vario-EL II element analyzer, and the percentage of the lanthanide cations were obtained by EDTA titrimetric analysis. IR spectra were recorded in the range of $4000\text{--}400\text{ cm}^{-1}$ on a Bruker TENSOR27 spectrometer using KBr medium pellets. The data of single crystal X-ray diffraction were collected on a smart-1000 diffractometer with graphite monochromatic Mo $\text{K}\alpha$ ($\lambda = 0.71073\text{ \AA}$) and Cu $\text{K}\alpha$ ($\lambda = 1.54178\text{ \AA}$) at 293(2) K. The structures were solved by SHELXS-97 program (direct methods) and refined by Full-matrix least-squares on F^2 using SHELXL-97 program.

The thermogravimetry (TG), derivative thermogravimetry (DTG), differential scanning calorimetric (DSC), was conducted using a TG/DSC system, which was a Netzsch STA 449 F3 instrument, under the simulated atmosphere (the gas flow rate of the nitrogen is 30 mL min^{-1} and the oxygen is 10 mL min^{-1}) with heat rate of 10 K min^{-1} from 299.15 to 1323.15 K. About 5 mg sample was weighed into an open alumina crucible.

The heat capacities of the title complexes were measured using a quantum design physical property measurement system (PPMS).

Synthesis of the title complexes

Two ligands of 2,3-DCIHBA (0.6 mmol) and 5,5'-dmebipy (0.2 mmol) were dissolved in ethanol (95%) together; the pH of the solution was adjusted to 6–7 with NaOH solution (1 mol L^{-1}). Then the mixed ligands solution was added to the $\text{LnCl}_3 \cdot \text{H}_2\text{O}$ (0.2 mmol) [$\text{Ln} = \text{Tb}(1), \text{Er}(2)$] aqueous solution under stirring. The mixed solution was stirred for 6 h and deposited for 12 h; the precipitates were filtered out and dried. After the volatilization of the mother liquor, single crystals of the title complexes were collected in two weeks at room temperature. Elemental analysis: calcd(%) for complex 1: C, 42.56; H, 2.27; N, 3.01; Tb, 17.06. Found(%): C, 42.65; H, 2.61; N, 2.79; Tb, 16.92. Calcd(%) for complex 2: C, 42.19; H, 2.25; N, 2.98; Er, 17.80. Found(%): C, 42.17; H, 2.48; N, 2.96; Er, 17.52.

Results and discussion

IR spectrum

The IR spectrum data of ligands and complexes are listed in Table 1. The complex 2 are discussed here as an example. Compared with the data of 2,3-DCIHBA, the characteristic absorption of $\nu_{\text{C=O}}$ (1692 cm^{-1}) disappears, and there are peaks of $\nu_{\text{sym}(\text{COO}^-)}$ and $\nu_{\text{asym}(\text{COO}^-)}$ at 1574 and 1410 cm^{-1} in the IR spectra of complex. The absorption of $\nu_{\text{Ln-O}}$ occurs at 419 cm^{-1} , indicating that lanthanide ion is coordinated to the oxygen atoms of the ligand [20]. The $\nu_{\text{C=N}}$ (1598 cm^{-1}) and $\delta_{\text{C-H}}$ ($828,737\text{ cm}^{-1}$) of 5,5'-dmebipy are shifted to $\nu_{\text{C=N}}$ (1659 cm^{-1}) and $\delta_{\text{C-H}}$ ($885,771\text{ cm}^{-1}$) in the IR spectra of complex, and this phenomenon also indicates the occurrence of coordination.

Crystal structure description

Data of crystallographic and refinement parameters of the complexes are shown in Table 2. The selected bond lengths and hydrogen bond lengths of the complexes are listed in Tables 3 and 4, respectively. Single crystal X-ray diffraction analysis of 1 and 2 reveals that they are isomorphous

Table 1 IR absorption bands for the ligands and complexes (cm^{-1})

Ligand/complexes	$\nu_{\text{C=N}}$	$\delta_{\text{C-H}}$	$\nu_{\text{C=O}}$	$\nu_{\text{sym}(\text{COO}^-)}$	$\nu_{\text{asym}(\text{COO}^-)}$	$\nu_{\text{Ln-O}}$
5,5'-dmebipy	1598	828,737	–	–	–	–
2,3-DCIHBA	–	–	1692	–	–	–
1	1647	883,771	–	1573	1410	420
2	1659	885,771	–	1574	1410	419

Table 2 Crystal data and structure refinement of the complexes

Complex	1	2
Empirical formula	C ₆₆ H ₄₆ C ₁₁₂ N ₄ O ₁₄ Tb ₂	C ₆₆ H ₄₆ C ₁₁₂ Er ₂ N ₄ O ₁₄
Formula weight	1862.31	1878.99
<i>T</i> /K	293(2)	293(2) K
Wavelength/Å	0.71073	1.54178
Crystal system	Triclinic	Triclinic
Space group	P $\bar{1}$	P $\bar{1}$
<i>a</i> /Å	11.1990(8)	11.2868(10)
<i>b</i> /Å	11.2601(9)	11.3246(12)
<i>c</i> /Å	15.2189(14)	15.1212(15)
α /°	93.6620(10)	94.1850(10)
β /°	99.140(2)	98.808(2)
γ /°	110.402(3)	111.487(3)
Volume/Å ³	1761.1(2)	1759.6(3)
<i>Z</i> , calculated density/Mg m ⁻³	1, 1.756	1, 1.773
Absorption coefficient/mm ⁻¹	2.513	9.047
<i>F</i> (000)	916	922
Crystal size/mm	0.23 × 0.18 × 0.08	0.26 × 0.17 × 0.07
θ range for data collection/°	2.61–25.02	2.99–66.20
Limiting indices	−12 ≤ <i>h</i> ≤ 13, −13 ≤ <i>k</i> ≤ 13, 17 ≤ <i>l</i> ≤ 18	−13 ≤ <i>h</i> ≤ 10, −9 ≤ <i>k</i> ≤ 13, −17 ≤ <i>l</i> ≤ 17
Reflections collected/unique	11552/6174 [<i>R</i> _(int) = 0.1475]	11,170/6150 [<i>R</i> _(int) = 0.1324]
Completeness to $\theta = 25.02$	99.1%	99.9%
Max. and min. transmission	0.8243 and 0.5956	0.5700 and 0.2020
Data/restraints/parameters	6174/0/444	6150/0/444
Goodness-of-fit on <i>F</i> ²	1.060	1.051
Final <i>R</i> indices [<i>I</i> > 2σ(<i>I</i>)]	<i>R</i> ₁ = 0.1047, <i>wR</i> ₂ = 0.1971	<i>R</i> ₁ = 0.0936, <i>wR</i> ₂ = 0.1927
<i>R</i> indices (all data)	<i>R</i> ₁ = 0.1660, <i>wR</i> ₂ = 0.2334	<i>R</i> ₁ = 0.1440, <i>wR</i> ₂ = 0.2396
Largest diff. peak and hole/e Å ⁻³	2.964 and −2.272	2.153 and −2.294

Table 3 Selected bond lengths (Å) of the complexes

Complex 1		Complex 2	
Tb(1)–O(5)	2.271(12)	Er(1)–O(3)	2.263(8)
Tb(1)–O(2)#1	2.319(10)	Er(1)–O(2)#1	2.296(9)
Tb(1)–O(1)	2.323(10)	Er(1)–O(1)	2.309(9)
Tb(1)–O(6)#1	2.390(11)	Er(1)–O(5)	2.358(9)
Tb(1)–O(3)	2.393(11)	Er(1)–O(7)	2.358(8)
Tb(1)–O(7)	2.405(10)	Er(1)–O(4)#1	2.363(9)
Tb(1)–N(2)	2.560(12)	Er(1)–N(2)	2.507(11)
Tb(1)–N(1)	2.608(14)	Er(1)–N(1)	2.549(12)

Symmetry transformations used to generate equivalent atoms: #1 $-x + 1, -y + 1, -z + 1$

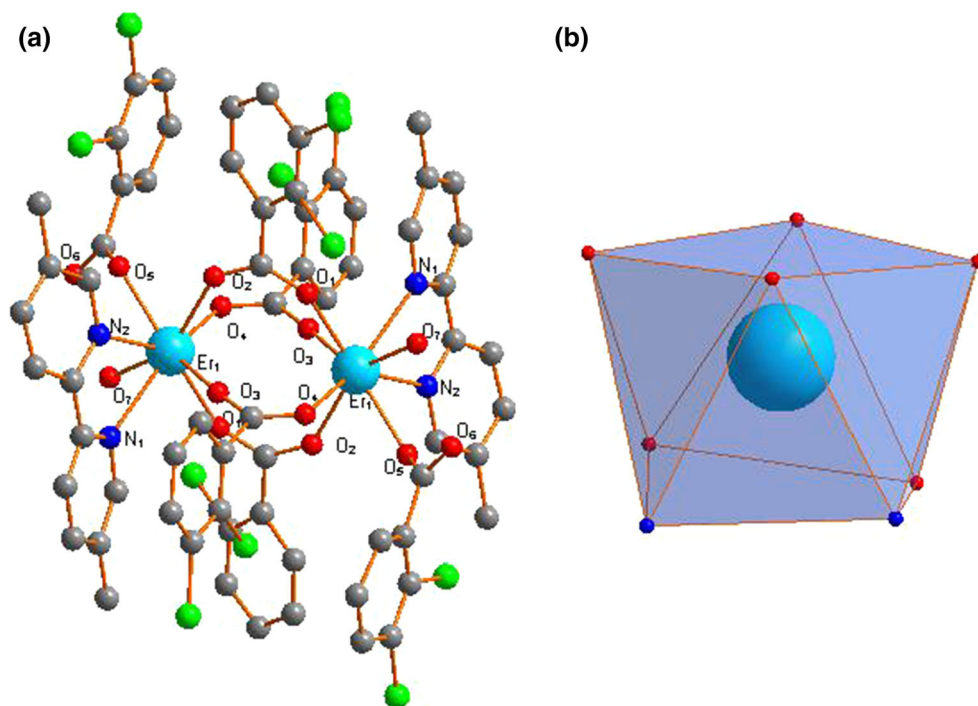
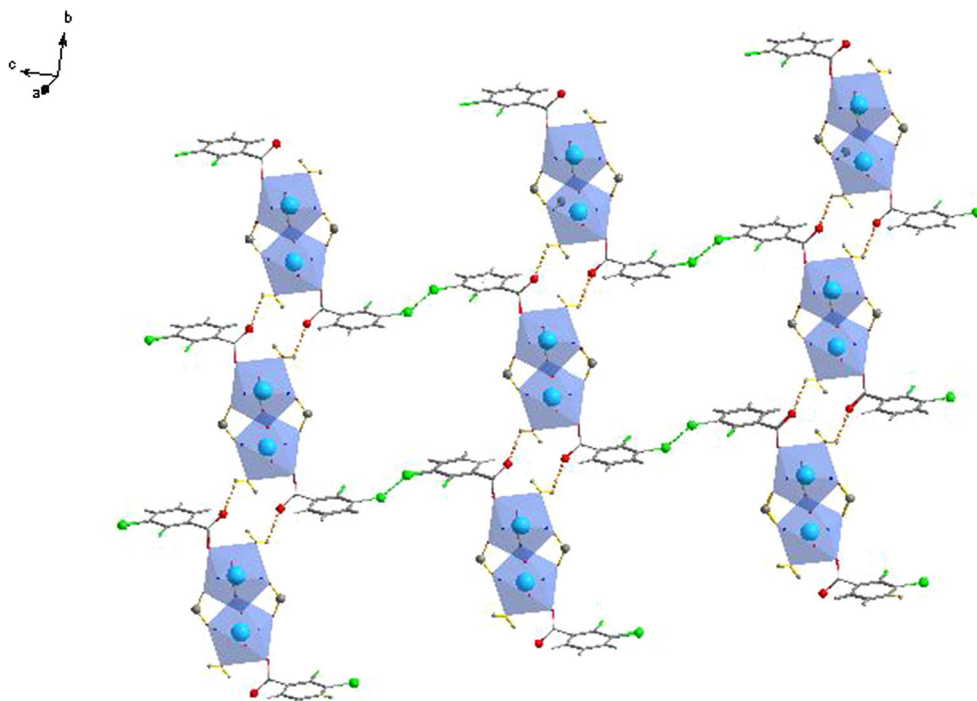
and crystallize in the same triclinic space group P $\bar{1}$. The crystal structure of complex 2 is described here in detail. The Er(III) ion center is eight coordinated with six oxygen atoms containing one O atom coming from the terminal

water molecule, one O atom coming from the acid ligand with monodentate mode, others belong to the ligand with bridging bidentate, and two nitrogen atoms from the coligand to furnish a square antiprism geometry (Fig. 1a, b). The average distance of Er–O_{carboxyl} is 2.318 Å, which is significantly shorter than that of Er–O_w bonds (2.358 Å), indicating that the water molecules are easy to lose.

The supramolecular architecture of the complex 2 is constructed by two non-covalent interactions as hydrogen bond and halogen–halogen interactions. The hydrogen bond interactions take place between the coordinated water and the monodentate oxygen atom along *b* axis to form a 1D chain. The 1D chain is connected by C–Cl \cdots C–Cl interactions with Cl₁–Cl₂ distance of 3.703 Å (Fig. 2) to construct three-dimensional supramolecular structure of the complex. In general, the intermolecular C–X₁ \cdots X₂–C interactions (X = F, Cl, Br, I) are classified into two types depending on the values of the angles $\theta_1 = \text{C–X}_1\cdots\text{X}_2$ and

Table 4 Selected hydrogen bond lengths (Å) of the complexes

Complexes	D–H...A	d(D–H)/Å	d(H...A)/Å	d(D...A)/Å	<DHA/°
1	O7–H7B...O4	0.850	1.813	2.629	160.35
	O7–H7C...O4	0.850	2.337	2.805	124.32
2	O7–H7B...O6	0.850	1.812	2.629	160.56
	O7–H7C...O6	0.850	2.333	2.847	119.29

Fig. 1 Crystal structure of the complex 2: **a** a independent structure unit, **b** a distorted capped square antiprism coordination polyhedron of Er (III) ion**Fig. 2** The 3D supramolecular architecture of complex 2 formed by H bond and halogen–halogen interactions (*red dotted lines* represent H bond, *green dotted lines* represent halogen–halogen interactions). (Color figure online)

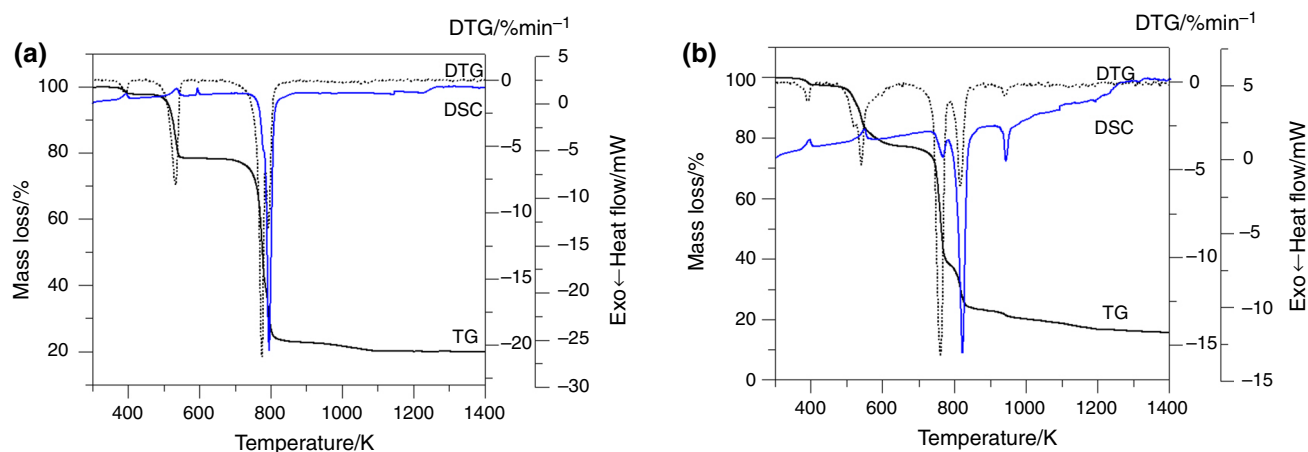


Fig. 3 TG–DTG/DSC curves of the complexes at the heating rate of 10 K min^{-1} (complex 1 **a**, complex 2 **b**)

Table 5 Thermal decomposition data of the title complexes ($\beta = 10 \text{ K min}^{-1}$)

Complex	Stage	Temperature range/K	DTG T_p /K	Mass loss/%		Probable removed groups	Main intermediate and final solid products
				Found	Calcd		
1	I	368.15–404.15	391.15	1.99	1.93	Coordinated water	$[\text{Tb}(2,3\text{-DCIBA})_3(5,5'\text{-dmebipy})]_2$
	II	464.15–664.15	541.15	19.95	19.78	2(5,5'-dmebipy)	$[\text{Tb}(2,3\text{-DCIBA})_3]_2$
	III	664.15–1323.15	760.75	61.00	58.21	6(2,3-DCIBA)	Tb_4O_7
				816.35			
				940.35			
				81.33 ^a	81.92		
2	I	366.15–411.15	388.65	1.98	1.92	Coordinated water	$[\text{Er}(2,3\text{-DCIBA})_3(5,5'\text{-dmebipy})]_2$
	II	467.15–683.15	526.45	19.64	19.61	2(5,5'-dmebipy)	$[\text{Er}(2,3\text{-DCIBA})_3]_2$
	III	683.15–1323.15	777.25	57.98	58.12	6(2,3-DCIBA)	Er_2O_3
				860.35			
				79.60 ^a	79.65		

β is heating rate. T_p is the peak temperature of DTG

^a The total loss rate

$\theta_2 = X_1 \cdots X_2 - C$. The interactions with similar angles ($\theta_1 = \theta_2$) are called Type I. On the other hand, the condition of $\theta_1 = 180^\circ$ and $\theta_2 = 90^\circ$ is satisfied for the interactions of Type II [21]. In the complex 2, the geometry of halogen–halogen interactions is characterized by $C_{18}-C_{16} \cdots Cl_6$ (θ_1) and $C_{18'}-Cl_{6'} \cdots Cl_6$ (θ_2) angles of 129.99° and 129.99° , respectively. The interaction is corresponding to halogen–halogen interaction of Type I.

Thermal decomposition mechanism

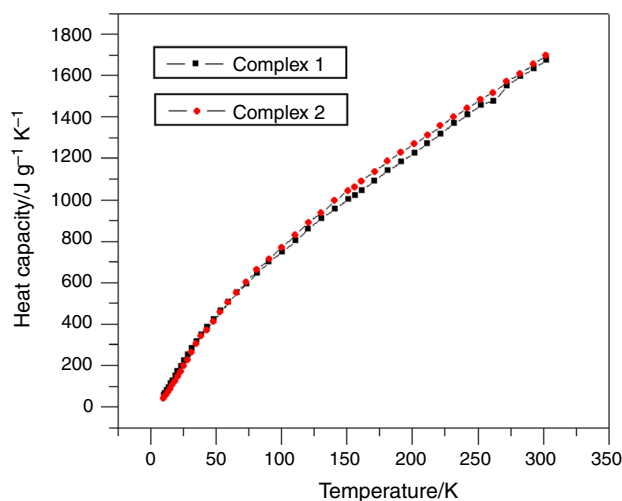
The thermogravimetric analysis of the complexes was performed in a dynamic simulated air atmosphere from 298.15 to 1323.15 K (Fig. 3) at a heating rate of 10 K min^{-1} . The data of thermal analysis for the complexes are listed in Table 5. The data of enthalpies and peak temperatures for the complexes are listed in Table 6.

Table 6 Enthalpies and peak temperatures for the title complexes from DSC analysis of TG/DSC system

complex	Stage	Temperature range/K	DSC peak Temperature/K	$\Delta H_m / \text{KJ mol}^{-1}$
1	I	368.15–404.15	392.15	112.08
	II	470.15–664.15	547.15	152.10
	III	664.15–1323.15	763.15	–331.50
			818.15	–8494.31
			940.15	–1641.69
2	I	366.15–411.15	390.15	106.07
	II	467.15–683.15	531.15	170.26
	III	683.15–1323.15	793.15	–7739.79

Table 7 Experimental molar heat capacities of the title complexes from (10 to 302) K

Complex 1		Complex 2	
T/K	$C_{p,m}/\text{J mol}^{-1} \text{K}^{-1}$	T/K	$C_{p,m}/\text{J mol}^{-1} \text{K}^{-1}$
10.15	56.40	10.12	42.39
11.25	67.02	11.22	51.35
12.49	78.77	12.46	61.89
13.86	93.34	13.83	74.13
15.38	109.55	15.35	88.19
17.07	127.76	17.02	104.18
18.95	148.34	18.91	122.82
21.04	170.76	21.00	143.18
23.35	195.47	23.29	166.05
25.91	222.76	25.87	192.73
28.78	250.80	28.73	220.35
31.94	281.58	31.90	252.84
35.47	314.61	35.34	292.02
39.38	349.20	39.21	328.01
43.70	385.94	43.62	356.00
48.50	422.86	48.43	396.19
53.82	463.01	53.78	437.62
59.73	506.38	59.69	482.17
66.31	551.32	66.27	529.16
73.62	596.19	73.58	577.35
81.72	646.84	81.68	632.06
90.70	699.50	90.68	683.56
100.65	746.78	100.62	736.56
110.79	801.83	110.76	793.48
120.83	860.42	120.80	850.16
130.92	907.81	130.88	894.53
141.01	954.40	140.96	948.83
151.16	1000.54	151.10	996.13
156.36	1019.01	156.34	1010.98
161.26	1045.84	161.24	1039.01
171.38	1091.31	171.33	1084.13
181.46	1140.38	181.45	1131.54
191.57	1183.55	191.52	1171.22
201.64	1223.20	201.64	1210.13
211.76	1271.44	211.75	1250.16
221.87	1320.04	221.87	1294.29
231.97	1367.04	231.99	1333.64
242.03	1411.48	242.03	1373.13
252.19	1459.20	252.19	1414.10
262.26	1474.97	262.25	1445.84
272.30	1548.07	272.27	1498.04
282.37	1594.48	282.35	1534.83
292.51	1632.38	292.49	1575.08
302.54	1677.36	302.55	1618.13

**Fig. 4** Experimental molar heat capacities of the title complexes from (10 to 302) K**Table 8** The fitted polynomial equations of the two complexes

Complex	Temperature range/K	Fitted polynomial equations
1	10.11–302.54	$C_{p,m}/\text{J mol}^{-1} \text{K}^{-1} = 1016.33895 + 657.86685x - 111.8896x^2 + 96.8168x^3 - 112.43989x^4 + 37.75898x^5 + 35.12513x^6$ $R^2 = 0.9999 \text{ SD} = 4.00$
2	10.14–302.54	$C_{p,m}/\text{J mol}^{-1} \text{K}^{-1} = 1023.34247 + 670.72894x - 50.89561x^2 + 87.22242x^3 - 106.27593x^4 + 55.99473x^5 - 1.08497x^6$ $R^2 = 0.9999 \text{ SD} = 4.93$

The complex 2 here will be discussed in detail since the two complexes have similar decomposition processes.

The TG curve in Fig. 3 shows that the complex 2 decomposes in three steps. The first stage mass loss of 1.98% takes place between 366.15 and 411.15 K corresponding to the loss of two coordinated water molecules (calcd: 1.92%). According to the DSC curve, a small endothermic peak ($T_p = 390.15 \text{ K}$; $\Delta H_m = 106.07 \text{ kJ mol}^{-1}$) appears in the first stage. The second stage has a mass loss of 19.64% which is attributed to the loss of 5,5'-dmebipy (calcd: 19.61%) in the temperature range of 467.15–683.15 K. Two endothermic peaks in the second stage on the DSC curve can be observed ($T_p = 531.15, 594.15 \text{ K}$; $\Delta H_m = 170.26, 62.22 \text{ kJ mol}^{-1}$). The third stage has a mass loss of 57.98% owing to the decomposition of 2,3-DCIBA ligands (calcd: 58.12%) from 683.15 to 1323.15 K, giving the final residual products of Er_2O_3 (found: 20.40%, calcd: 20.36%). There are two strong exothermic peaks ($T_p = 793.15 \text{ K}$; $\Delta H_m = -7739.79 \text{ kJ mol}^{-1}$) in the last stage on the DSC curve. In

Table 9 Standard thermodynamic functions of the complexes

Complex 1				Complex 2			
<i>T</i> /K	$C_{p,m}/$ $J K^{-1} mol^{-1}$	$H_T - H_{298.15K}/$ $KJ mol^{-1}$	$S_T - S_{298.15K}/$ $J k^{-1} mol^{-1}$	<i>T</i> /K	$C_{p,m}/$ $J K^{-1} mol^{-1}$	$H_T - H_{298.15K}/$ $KJ mol^{-1}$	$S_T - S_{298.15K}/$ $J k^{-1} mol^{-1}$
10.14	51.14	-280.687	-1971.48	10.11	34.69	-274.135	-1971.48
15.14	109.10	-280.285	-1940.04	15.11	88.33	-273.827	-1875.70
20.14	163.75	-279.602	-1901.40	20.11	139.85	-273.256	-1843.39
25.14	215.32	-278.653	-1859.53	25.11	189.32	-272.432	-1807.01
30.14	264.06	-277.454	-1816.15	30.11	236.82	-271.366	-1768.42
35.14	310.17	-276.017	-1772.14	35.11	282.40	-270.067	-1728.61
40.14	353.86	-274.356	-1728.01	40.11	326.16	-268.546	-1688.14
45.14	395.33	-272.483	-1684.06	45.11	368.16	-266.809	-1647.39
50.14	434.76	-270.407	-1640.48	50.11	408.50	-264.867	-1606.59
55.14	472.33	-268.139	-1597.38	55.11	447.25	-262.727	-1565.91
60.14	508.20	-265.687	-1554.83	60.11	484.51	-260.397	-1525.47
65.14	542.52	-263.060	-1512.88	65.11	520.36	-257.885	-1485.33
70.14	575.43	-260.264	-1471.55	70.11	554.87	-255.196	-1445.56
75.14	607.07	-257.308	-1430.84	75.11	588.15	-252.339	-1406.20
80.14	637.56	-254.196	-1390.76	80.11	620.26	-249.317	-1367.26
85.14	667.02	-250.934	-1351.28	85.11	651.30	-246.138	-1328.77
90.14	695.56	-247.527	-1312.41	90.11	681.33	-242.806	-1290.74
95.14	723.27	-243.980	-1274.11	95.11	710.45	-239.327	-1253.16
100.14	750.24	-240.296	-1236.38	100.11	738.71	-235.704	-1216.04
105.14	776.57	-236.479	-1199.18	105.11	766.19	-231.941	-1179.37
110.14	802.32	-232.532	-1162.51	110.11	792.96	-228.043	-1143.14
115.14	827.56	-228.457	-1126.33	115.11	819.08	-224.013	-1107.35
120.14	852.37	-224.257	-1090.63	120.11	844.61	-219.853	-1071.98
125.14	876.79	-219.934	-1055.37	125.11	869.60	-215.568	-1037.03
130.14	900.89	-215.490	-1020.55	130.11	894.11	-211.158	-1002.47
135.14	924.70	-210.926	-986.14	135.11	918.18	-206.628	-968.30
140.14	948.26	-206.244	-952.12	140.11	941.86	-201.978	-934.51
145.14	971.62	-201.444	-918.47	145.11	965.17	-197.210	-901.07
150.14	994.80	-196.528	-885.17	150.11	988.17	-192.327	-867.99
155.14	1017.83	-191.497	-852.20	155.11	1010.86	-187.329	-835.24
160.14	1040.74	-186.350	-819.56	160.11	1033.30	-182.219	-802.81
165.14	1063.55	-181.090	-787.21	165.11	1055.48	-176.997	-770.70
170.14	1086.27	-175.715	-755.15	170.11	1077.44	-171.664	-738.88
175.14	1108.91	-170.227	-723.36	175.11	1099.19	-166.223	-707.36
180.14	1131.49	-164.626	-691.83	180.11	1120.74	-160.673	-676.11
185.14	1154.02	-158.913	-660.54	185.11	1142.10	-155.016	-645.13
190.14	1176.50	-153.086	-629.49	190.11	1163.28	-149.253	-614.40
195.14	1198.94	-147.148	-598.66	195.11	1184.28	-143.384	-583.93
200.14	1221.34	-141.097	-568.05	200.11	1205.12	-137.410	-553.70
205.14	1243.71	-134.935	-537.63	205.11	1225.79	-131.333	-523.71
210.14	1266.04	-128.661	-507.42	210.11	1246.30	-125.153	-493.94
215.14	1288.35	-122.275	-477.38	215.11	1266.64	-118.871	-464.39
220.14	1310.62	-115.777	-447.53	220.11	1286.84	-112.487	-435.05
225.14	1332.87	-109.169	-417.85	225.11	1306.89	-106.003	-405.92
230.14	1355.09	-102.449	-388.33	230.11	1326.79	-99.418	-376.99
235.14	1377.28	-95.618	-358.96	235.11	1346.57	-92.735	-348.26

Table 9 continued

Complex 1				Complex 2			
<i>T</i> /K	<i>C</i> _{p,m} / J K ⁻¹ mol ⁻¹	<i>H</i> _T - <i>H</i> _{298.15K} / KJ mol ⁻¹	<i>S</i> _T - <i>S</i> _{298.15K} / J k ⁻¹ mol ⁻¹	<i>T</i> /K	<i>C</i> _{p,m} / J K ⁻¹ mol ⁻¹	<i>H</i> _T - <i>H</i> _{298.15K} / KJ mol ⁻¹	<i>S</i> _T - <i>S</i> _{298.15K} / J k ⁻¹ mol ⁻¹
240.14	1399.45	-88.676	-329.75	240.11	1366.24	-85.953	-319.72
245.14	1421.61	-81.624	-300.68	245.11	1385.82	-79.073	-291.36
250.14	1443.76	-74.461	-271.76	250.11	1405.34	-72.095	-263.18
255.11	1424.82	-65.020	-235.17	255.11	1424.82	-65.020	-235.17
260.11	1444.30	-57.847	-207.32	260.11	1444.30	-57.847	-207.32
265.11	1463.85	-50.577	-179.64	265.11	1463.85	-50.577	-179.64
270.11	1483.50	-43.209	-152.10	270.11	1483.50	-43.209	-152.10
275.11	1503.34	-35.742	-124.71	275.11	1503.34	-35.742	-124.71
280.11	1523.43	-28.175	-97.45	280.11	1523.43	-28.175	-97.45
285.11	1543.88	-20.507	-70.32	285.11	1543.88	-20.507	-70.32
290.11	1564.79	-12.736	-43.30	290.11	1564.79	-12.736	-43.30
295.11	1586.27	-4.859	-16.38	295.11	1586.27	-4.859	-16.38
300.11	1608.48	3.160	10.56	300.11	1608.48	3.160	10.56

addition, the IR spectrum of the residues is the same to that of the sample Er₂O₃.

Heat capacity

The molar heat capacities for the title complexes are listed in Table 7, and the relationship of molar heat capacities to temperature is plotted in Fig. 4. It can be seen that the heat capacity gradually increases with temperature, and no phase transition or thermal anomalies are observed across the whole temperature range. We can conclude that the complexes are thermodynamically stable over the temperature range from (10 to 302) K. The experimental heat capacities and the reduced temperature (*x*) were fitted to the polynomial equations by a least square method. The reduced temperature was calculated by the equation, $x = [T - (T_{\max} + T_{\min})/2]/[(T_{\max} - T_{\min})/2]$, where *T* is the experimental temperature, *T*_{max} and *T*_{min} are the upper and lower limits, respectively. The correlation coefficient (*R*²) and standard deviation (SD) were obtained. The fitted polynomial equations are shown in Table 8.

Based on the fitted polynomial and thermodynamic equations, the smoothed heat capacities and thermodynamic functions of the complexes were calculated. The thermodynamic equations are as follows. The results are shown in Table 9.

$$H_T - H_{298.15K} = \int_{298.15K}^T C_{p,m} dT \quad (1)$$

$$S_T - S_{298.15K} = \int_{298.15K}^T C_{p,m} T^{-1} dT \quad (2)$$

Conclusions

In summary, the synthesis and characterization of two novel complexes [Tb(2,3-DCIBA)₃(5,5'-dmebipy)(H₂O)]₂ and [Er(2,3-DCIBA)₃(5,5'-dmebipy)(H₂O)]₂ were reported. The hydrogen bond and halogen-halogen interactions in the complex can construct supramolecular. According to TG/DSC technology, thermal decomposition process of the complexes has been obtained. The coordinated water molecules lose first, then 5,5'-dmebipy ligands, and finally the 2,3-DCIBA ligands begin to decompose. The experimental data of low-temperature heat capacities were fitted to the polynomial equations by a least square method, and the thermodynamic functions were calculated based on the curve fitting.

Supplementary material

The numbers of the complexes (CCDC 1409261(1) 1409257(2)) contain the supplementary crystallographic data for this paper, which can be obtained free of charge from the Cambridge Crystallographic Data Centre via www.ccdc.cam.ac.uk/data_request/cif.

Acknowledgements The research work is supported by the National Natural Science Foundation of China (Nos. 21473049 and 21473198) and the Natural Science Foundation of Hebei Province (No. B2016205207).

References

1. Zhu Y, Wang YM, Xu J, Liu P, Weththasinha HABMD, Wu YL, Lu XQ, Xie JM. Syntheses, structures, molecular and cationic recognitions and catalytic properties of two lanthanide coordination polymers based on a flexible tricarboxylate. *J Solid State Chem.* 2014;219:259–64.
2. Fang QR, Zhu GS, Jin Z, Ji YY, Ye JW, Xue M, Yang H, Wang Y, Qiu SL. Mesoporous metal–organic framework with rare etb topology for hydrogen storage and dye assembly. *Angew Chem.* 2007;46:6638–42.
3. Yang AH, Zou JY, Wang WM, Shi XY, Gao HL, Cui JZ, Zhao B. Two three-dimensional lanthanide frameworks exhibiting luminescence increases upon dehydration and novel water layer involving in situ decarboxylation. *Inorg Chem.* 2014;53:7092–100.
4. Marques LF, Dos Santos MV, Ribeiro SJL, Castellano EE, Machado FC. Terbium(III) and dysprosium(III) 8-connected 3D networks containing 2,5-thiophenedicarboxylate anion: crystal structures and photoluminescence studies. *Polyhedron.* 2012;38:149–56.
5. Xu J, Sun LB, Xing HZ, Liang ZQ, Yu JH, Xu RR. A new lanthanide metal–organic framework with (3,6)-connected topology based on novel tricarboxylate ligand. *Inorg Chem Commun.* 2011;14:978–81.
6. Evans RC, Douglas P, Winscom CJ. Coordination complexes exhibiting room-temperature phosphorescence: evaluation of their suitability as triplet emitters in organic light emitting diodes. *Coord Chem Rev.* 2006;250:2093–126.
7. Zhou YS, Li XM, Zhang LJ, Guo Y, Shi ZH. 3-D silver(I)—lanthanide(III) heterometallic-organic frameworks constructed from 2,2'-bipyridine-3,3'-dicarboxylic acid: synthesis, structure, photoluminescence, and their remarkable thermostability. *Inorg Chem.* 2014;53:3362–70.
8. Sivakumar S, Reddy MLP. Bright green luminescent molecular terbium plastic materials derived from 3,5-bis(perfluorobenzyloxy)benzoate. *J Mater Chem.* 2012;22:10852–9.
9. Eliseeva SV, Bunzli JCG. Lanthanide luminescence for functional materials and bio-sciences. *Chem Soc Rev.* 2010;39:189–227.
10. Biju S, Gopakumar N, Bunzli JCG, Scopelliti R, Kim HK, Reddy MLP. Brilliant photoluminescence and triboluminescence from ternary complexes of DyIII and TbIII with 3-Phenyl-4-propanoyl-5-isoxazolonate and a bidentate phosphine oxide coligand. *Inorg Chem.* 2013;52:8750–8.
11. Kido J, Okamoto Y. Organo lanthanide metal complexes for electroluminescent materials. *Chem Rev.* 2002;102:2357–68.
12. Caires FJ, Gomes DJC, Gigante AC, Ionashiro M. Thermal investigation and infrared evolved gas analysis of solid trivalent lanthanide and yttrium alpha-hydroxyisobutyrate in N₂ and CO₂ atmospheres. *J Anal Appl Pyrolysis.* 2014;107:313–22.
13. Xu N, Wang C, Shi W, Yan SP, Cheng P, Liao DZ. Magnetic and luminescent properties of Sm, Eu, Tb, and Dy coordination polymers with 2-hydroxynicotinic acid. *Eur J Inorg Chem.* 2011;2011:2387–93.
14. Goura J, Walsh JPS, Tuna F, Chandrasekhar V. Tetranuclear lanthanide(III) complexes in a seesaw geometry: synthesis, structure, and magnetism. *Inorg Chem.* 2014;53:3385–91.
15. Feng X, Liu L, Wang LY, Song HL, Shi ZQ, Wu XH, Ng SW. Lanthanide coordination polymers based on multi-donor ligand containing pyridine and phthalate moieties: structures, luminescence and magnetic properties. *J Solid State Chem.* 2013;206:277–85.
16. Arauzo A, Lazarescu A, Shova S, Bartolome E, Cases R, Luzon J, Bartolome J, Turta C. Structural and magnetic properties of some lanthanide (Ln = Eu(III), Gd(III) and Nd(III)) cyanoacetate polymers: field-induced slow magnetic relaxation in the Gd and Nd substitutions. *Dalton Trans.* 2014;43:12342–56.
17. Yang L, Liu L, Wu L, Xu Z, Wang L. Isomorphous and isostructural lanthanide coordination polymers based on 2-(4-chlorobenzoyl)benzoic acid: synthesis, structure, characterization, and luminescent properties. *Dyes Pigment.* 2014;111:176–84.
18. Jin CW, Shen PP, Ren N, Geng LN, Zhang JJ. Structure, luminescent and thermal properties of two novel lanthanide complexes with 3,4-diethoxybenzoic acid and 5,50-dimethyl-2,20-bipyridine. *J Therm Anal Calorim.* 2016;126:1549–58.
19. Wang Y, Zhao QQ, Ren N, Zhang JJ, Geng LN, Wang SP. Crystal structures, thermal properties, and luminescent properties of two novel mononuclear lanthanide complexes with 2,4-dichlorobenzoic acid and 2,2',6',2''-terpyridine. *J Therm Anal Calorim.* 2016;126:1703–12.
20. Wang JF, Meng FT, Xu SL, Liu X, Zhang JJ. Preparation, luminescence and thermal properties of lanthanide complexes with 2-chloro-4-fluorobenzoic acid. *Thermochim Acta.* 2011;521:2–8.
21. Kastan G, Albayrak C, Odabasoglu M, Frank R. Single stranded helical chains of C–H⋯π interactions further connected by halogen–halogen interactions of type I to construct supramolecular structure of (E)-5-(diethylamino)-2-[(4-iodophenylimino)methyl]phenol compound. *Spectrochim Acta A Mol Biomol Spectrosc.* 2012;94:200–4.